Taylor & Francis
Taylor & Francis Group

Numerical Heat Transfer, Part A: Applications
An International Journal of Computation and Methodology

ISSN: 1040-7782 (Print) 1521-0634 (Online) Journal homepage: www.tandfonline.com/journals/unht20

Implicit finite difference simulations for unsteady oscillating flow of Walters-B nanofluid with microbes using the Cattaneo–Christov model

Sami Ullah Khan, Adnan, Arshad Riaz, Katta Ramesh, M. M. Bhatti & Muhammad Awais

To cite this article: Sami Ullah Khan, Adnan, Arshad Riaz, Katta Ramesh, M. M. Bhatti & Muhammad Awais (31 Jul 2024): Implicit finite difference simulations for unsteady oscillating flow of Walters-B nanofluid with microbes using the Cattaneo–Christov model, Numerical Heat Transfer, Part A: Applications, DOI: 10.1080/10407782.2024.2383843

To link to this article: https://doi.org/10.1080/10407782.2024.2383843

Published online: 31 Jul 2024.

NUMERICAL HEAT TRANSFER, PART A: APPLICATIONS
https://doi.org/10.1080/10407782.2024.2383843

Implicit finite difference simulations for unsteady oscillating flow of Walters-B nanofluid with microbes using the Cattaneo–Christov model

Sami Ullah Khan[a], Adnan[b], Arshad Riaz[c], Katta Ramesh[d,e], M. M. Bhatti[f], and Muhammad Awais[g,h,i]

[a]Department of Mathematics, Namal University, Mianwali, Pakistan; [b]Department of Mathematics, Mohi-ud-Din Islamic University, Islamabad, Pakistan; [c]Department of Mathematics, Division of Science and Technology, University of Education, Lahore, Pakistan; [d]Department of Pure and Applied Mathematics, School of Mathematical Sciences, Sunway University, Selangor Darul Ehsan, Malaysia; [e]Department of Mathematics, Graphic Era (Deemed to be University), Dehradun, India; [f]Material Science Innovation and Modelling (MaSIM) Research Focus Area, North-West University (Mafikeng Campus), Mmabatho, South Africa; [g]Department of Electrical Engineering, Henan Agricultural University, Zhengzhou, China; [h]Henan International Joint Laboratory of Laser Technology in Agriculture Science, Zhengzhou, China; [i]State Key Laboratory of Wheat and Maize Crop Science, Zhengzhou, China

ABSTRACT

The thermal importance of nanoparticles in different fields of engineering is still a developing issue that necessitates additional focused consideration. The suspension of non-Newtonian fluids with nonmaterials has various applications in areas such as enhanced thermal systems, energy processes, aerospace engineering, and chemical industries. Following such motivations, this work aims to analyze the heat and mass transfer flow of Walters-B nanofluid in the presence of microorganisms. The fluid motion is presumed to be non-steady over a surface that undergoes periodic acceleration. The motivations for studying nanofluid's oscillating flow are its use in effective mixing processes, combustion stability, and process efficiency. The text provides a detailed explanation of the saturation of porous media. A modified theory for heat and mass fluxes, known as the Cattaneo–Christov approach, suggests an extension in heat equations. Moreover, it supports the interaction of radiation phenomena for enhancing heat transfer. It is noteworthy that the entire problem is represented using extremely nonlinear partial differential equations (PDEs). The CFD study utilizing the renowned implicit finite difference method (FDM) has been effectively employed to propose a numerical solution for the problem. The numerical results are deemed valid and confirmed within certain limiting cases, based on the available data. The evaluation of velocity, skin friction coefficient, Nusselt number, and Sherwood number as a function of time has been demonstrated for various parameters. It is asserted that the wall shear force exhibited an oscillating pattern with a greater magnitude as a result of the viscoelastic parameter. The Nusselt number and Sherwood number exhibit slight acceleration as a result of changes in the Prandtl number and Schmidt number, respectively. The proposed model is specifically designed for use in heat exchangers, vibrational systems, compact designs, and vibration control.

ARTICLE HISTORY
Received 29 May 2024
Revised 15 July 2024
Accepted 19 July 2024

KEYWORDS
Cattaneo–Christov model; implicit finite difference scheme; microbes; periodically oscillating flow; Walters-B nanofluid

CONTACT M. M. Bhatti mubashirme@hotmail.com; mmbhatti@sdust.edu.cn Material Science Innovation and Modelling (MaSIM) Research Focus Area, North-West University (Mafikeng Campus), Mmabatho, South Africa

1. Introduction

Nanomaterials are colloidal suspensions consisting of nanoparticles dispersed in a base fluid. Nanoparticles, such as carbides, metals, carbon nanotubes, and oxides, have a significant impact on the thermal characteristics of base liquids. The enhanced thermal properties can be attributed to the increased surface area of the nanoparticles and the improved stability of the colloid. Multiple eras of engineering have involved the utilization of nanofluids in automotive engines, chemical reactors, electronic devices, and other applications. Nanofluids have been found to have promising applications in the biomedical field, particularly in medication delivery and hyperthermia cancer therapies. The employment of nanoparticles allows for the effective observation of thermal energy and the increase of heat transport on the nanoscale. Nanofluids play a crucial function in solar systems and energy devices. Heat exchangers, nuclear reactors, automotive cooling, solar radiation, lubricants, and other systems also rely on nanofluids for their significance. In biomedical sciences, the significance of nanoparticles is attributed to medical imaging, the treatment of cancer, hyperthermia, etc. In recent times, there has been a wide range of literature dedicated to the examination of nanofluids. Wang *et al.* [1] provided a comprehensive analysis of the progress and durability of nanofluids. Mondal *et al.* [2] emphasized the potential benefits of using nanofluids for transporting fluids across porous materials, particularly in relation to the effects of uneven heating. Oudina *et al.* [3] proposed enhancing heat transmission by utilizing the interaction of magnetite nanoparticles. The analysis was conducted using the Buongiorno model. Nadeem *et al.* [4] used the Reynolds nanofluid model to predict the thermal consequences of Casson nanofluid on a slandering surface. Basit *et al.* [5] quantitatively investigate the Lorentz force in the nanofluid problem. Acharya *et al.* [6] conducted an experiment on the effects of iron oxide nanoparticles on chamber flow and obtained the findings. Irfan and Bhatti [7] anticipated the limitations on slip in order to investigate the reduction in heat transmission caused by nanofluid truncation. Khan *et al.* [8] conducted an investigation on the flow of Powell–Eyring nanofluid in an axisymmetric channel. Abdelsalam *et al.* [9] addressed the implementation of Sutterby nanofluid in hyperthermia therapeutic applications. Raza *et al.* [10] examined the utilization of Jeffrey nanofluid in a porous channel using fractional calculations. Kumar *et al.* [11] conducted an investigation of entropy and the significance of Bejan theory in relation to the flow of nanofluids. Sheikholeslami *et al.* [12] addressed the enhancement of heat transfer in thermoelectric generators with the use of nanoparticles. Bakar *et al.* [13] developed a slip model for nanofluid that accounts for the bioconvective phenomenon. Yaari *et al.* [14] made predictions on the use of nanomaterials in oil recovery in the presence of heterogeneous porous spaces. Gholizadeh *et al.* [15] conducted an experimental investigation on the importance of heat exchangers using nanofluids. Shahlaei *et al.* [16] examined the augmentation of heat transfer caused by the presence of nanofluid in the presence of Joule heating effects. Ghadikolaei *et al.* [17] indicated that they examined the thermal efficiency of an environmentally friendly nanofluid using a combination of passive methods. Bhatti *et al.* [18] investigated the electromagnetohydrodynamic (EMHD) convective transport of a reactive, dissipative Carreau fluid with thermal ignition in a non-Darcian vertical duct and presented numerical solutions. Bilal *et al.* [19] reported a study on the flow of nanofluid on a Riga surface, considering the effects of heat source and activation energy. Issakhov *et al.*, [20] assessed the natural convective flow in a cubic container that was filled with nanofluid.

Non-Newtonian materials are anticipated to have a pivotal impact on various fields including pharmaceuticals, cosmetics, food processing, polymers, and engineering. The intriguing characteristic of non-Newtonian materials is their varied change in viscosity when subjected to shear rate. Essentially, the varied characteristics of non-Newtonian fluids have been considered. Due to the unique characteristics of these materials, other types and categories have been suggested, such as shear thinning, dilatant, Bingham plastic, and viscoelastic materials. Non-Newtonian materials, like blood, are used in diagnostic and research applications in the medical industry. The Walters-

B model is a type of viscoelastic fluid that describes the relationship between shear force and deformation rate. The Walters-B model accurately characterizes the polymer-like properties of a fluid, in which the presence of long chain molecules imparts distinct rheological characteristics. These polymeric liquids are commonly used in the fields of biotechnology and chemical engineering. The original model for Walters-B fluid is attributed to the work of Bear and Walters [21], in which the governing equations were effectively established.

Pasha *et al.* [22] employed a computational method to study the behavior of Walters-B nanofluid in the presence of chemically reactive species. Rai *et al.* [23] applied the thermal instability framework to study the behavior of Walters-B viscoelastic nanofluid in Hele–Shaw cells. Vyakaranam *et al.* [24] examined the combined rheology of Walters-B nanofluid and tangent hypobaric fluid in the presence of thermos-diffusion phenomena. Smida *et al.* [25] investigated the use of Walters-B nanofluid for heat transmission in lubricated space. Sandeep *et al.* [26] conducted a study on slip flow using Walters-B nanofluid flow with heat transfer. Wang *et al.* [27] conducted a 3D investigation of the Walters-B nanofluid by introducing minuscule nanoparticles. Saini *et al.* [28] highlighted the significance of radiative phenomenon in relation to Walters-B fluid with porous space.

The Cattaneo–Christov (CC) heat flow model is a contemporary method used to alter the heat equation in the analysis of heat transport problems. The CC hypothesis is essentially an expansion of Fourier's law. Essentially, Fourier's model is linked to the concept of heat propagating at an unlimited speed, which frequently leads to predictions that are not in line with physical reality. Incorporating thermal relaxation time elements enhances the realism of the execution of the CC technique. The CC model is commonly used in engineering, geophysics, and other fields to address various thermal issues and optimize thermal management. References [29–32] contain several papers that have utilized the CC model for implementation.

According to purported scientific discoveries, it has been observed that several investigations on nanofluids have been carried out in various flow configurations. However, the unstable and periodically fluctuating bioconvective flow of Walter's B nanofluid, with the implementation of the modified CC model, has not been asserted or proven. The research endeavor seeks to study the thermally saturated flow of Walters-B nanofluid with a suspension of microorganisms under regularly oscillating conditions. This study investigates the examination of heat and mass transmission phenomena for a bioconvective Walters-B nanofluid across a porous, oscillating stretched surface. The examination of heat and mass transmission is associated with the use of the CC method. The inclusion of thermal radiation and heat sources is accounted for. The subject matter is exclusively approached *via* the use of partial differential equations (PDEs) instead of ordinary differential equations (ODEs). An implicit finite difference technique is used to find the numerical solution of these PDEs. The tangible components of the issue have been determined based on the given criteria. The reported findings of each flow parameter have been used to support claims of industrial and technical applications.

2. Statement of problem

Consider an unsteady two-dimensional (2-D) flow of Walters-B nanofluid with microbe suspension caused by a stretched surface that oscillates uniformly. The sheet endorsed the flow with velocity $u = u_{\omega} = bx \sin \varpi t$ for which b and ϖ provides the illustration of stretching rate and angular frequency, respectively. The convective boundary conditions are used to evaluate the flow of heat and mass transfer. Porous space is maintained permeability by its oscillating surface. The flow problem is modeled in coordinate system where x is taken along the stretching surface while y is oriented in normal to surface. The focus is on the assumptions made about the normal magnetic field. Using a modified approach, the heat equation is updated with the CC method. In addition, the potential effects of radiation and heat sources are being considered. The velocity component u is along horizontal axis while v is taken in vertical direction to the plate. The problem has been formulated based on the following equations [33–35]:

$$\frac{\partial u}{\partial x}+\frac{\partial v}{\partial y}=0, \tag{1}$$

$$\frac{\partial u}{\partial t}+u\frac{\partial u}{\partial x}+v\frac{\partial u}{\partial y}=\nu\frac{\partial^2 u}{\partial y^2}-\Gamma\left[\begin{array}{l}\frac{\partial^3 u}{\partial t\partial y^2}+u\frac{\partial^3 u}{\partial x\partial y^2}+v\frac{\partial^3 u}{\partial y^3}\\ +\frac{\partial u}{\partial x}\frac{\partial^2 u}{\partial y^2}-\frac{\partial u}{\partial y}\frac{\partial^2 u}{\partial x\partial y}\end{array}\right]-\frac{\sigma B_0^2}{\rho_f}u-\frac{\varphi}{\Omega}\left(\nu+\Gamma\frac{\partial}{\partial t}\right)u, \tag{2}$$

$$\begin{aligned}\frac{\partial T}{\partial t}+u\frac{\partial T}{\partial x}+v\frac{\partial T}{\partial y}+A_T\left[\begin{array}{l}\frac{\partial^2 T}{\partial t^2}+2u\frac{\partial^2 T}{\partial x\partial t}+2v\frac{\partial^2 T}{\partial y\partial t}\\ +\frac{\partial v}{\partial t}\frac{\partial T}{\partial y}+u\frac{\partial u}{\partial x}\frac{\partial T}{\partial x}+v\frac{\partial v}{\partial y}\frac{\partial T}{\partial y}\\ +u\frac{\partial v}{\partial x}\frac{\partial T}{\partial y}+v\frac{\partial u}{\partial y}\frac{\partial T}{\partial x}\\ +2uv\frac{\partial^2 T}{\partial x\partial y}+u^2\frac{\partial^2 T}{\partial x^2}+v^2\frac{\partial^2 T}{\partial y^2}\end{array}\right]&=\left(\Lambda+\frac{16\varepsilon T_\infty^3}{3k_a(\rho c)_f}\right)\frac{\partial^2 T}{\partial y^2}+\frac{Q}{(\rho c)_f}(T-T_f)\\ &+\Upsilon\left[\frac{D_B}{\Delta C}\frac{\partial C}{\partial y}\frac{\partial T}{\partial y}+\frac{D_T}{T_\infty}\left(\frac{\partial T}{\partial y}\right)^2\right],\end{aligned} \tag{3}$$

$$\frac{\partial C}{\partial t}+u\frac{\partial C}{\partial x}+v\frac{\partial C}{\partial y}+B_C\left[\begin{array}{l}\frac{\partial^2 C}{\partial t^2}+2u\frac{\partial^2 C}{\partial x\partial t}+2v\frac{\partial^2 C}{\partial y\partial t}\\ +\frac{\partial v}{\partial t}\frac{\partial C}{\partial y}+u\frac{\partial u}{\partial x}\frac{\partial C}{\partial x}+v\frac{\partial v}{\partial y}\frac{\partial C}{\partial y}\\ +u\frac{\partial v}{\partial x}\frac{\partial C}{\partial y}+v\frac{\partial u}{\partial y}\frac{\partial C}{\partial x}\\ +2uv\frac{\partial^2 C}{\partial x\partial y}+u^2\frac{\partial^2 C}{\partial x^2}+v^2\frac{\partial^2 C}{\partial y^2}\end{array}\right]=D_B\frac{\partial^2 C}{\partial y^2}+\frac{D_T}{T_\infty}\frac{\partial^2 T}{\partial y^2}, \tag{4}$$

$$\frac{\partial \psi}{\partial t}+u\frac{\partial \psi}{\partial x}+v\frac{\partial \psi}{\partial y}+\frac{\vartheta w}{(C_w-C_\infty)}\left[\frac{\partial}{\partial y}\left(\psi\frac{\partial C}{\partial y}\right)\right]=D_m\left(\frac{\partial^2\psi}{\partial y^2}\right), \tag{5}$$

where t is the time, ν exposes the dynamic viscosity, Γ is viscoelastic coefficient, σ electrical conducting, φ porous medium, Ω permeability of porous space, B_0 magnetic force strength, A_T is the coefficient of thermal relaxation time, B_C is for concentration relaxation coefficient, T is for temperature, Λ be thermal diffusivity, Q external heat source, D_T is thermophoresis factor, T_f convective heat transfer, C is concentration, Υ is ratio of capacitance of nanofluid to base fluid particles, D_B be Brownian diffusion, D_B is Brownian factor, ψ microbe's density, ε denotes the Boltzmann constant, k_a is for mean absorption coefficient, ϑ chemotaxis coefficient, w defining the speed associated to swimming cells, and D_m microorganisms diffusion constant.

The problem is being considered in the light of the following conditions [35]:

$$\left.\begin{aligned}&u=u_\omega=bx\sin\varpi t,\quad v=0,\quad -k\frac{\partial T}{\partial y}=h_f\left(T_f-T\right),\quad -D_B\frac{\partial C}{\partial y}=k_f(C_f-C),\psi=\psi_w\quad\text{at}\quad y=0,\qquad t>0,\\&u\to 0,\quad \frac{\partial u}{\partial y}\to 0,\quad T\to T_\infty,\ C\to C_\infty,\ \psi\to\psi_\infty\quad\text{at}\quad y\to\infty.\end{aligned}\right\}\tag{6}$$

where h_f is heat transfer coefficient while k_f reflects the coefficient of mass transfer. Since the flow induced in unbounded domain therefore, the augmented constraints $\frac{\partial u}{\partial y}\to 0$ is implemented. Let the suggesting new variables for simplifying the problem [34, 35]:

$$\left.\begin{aligned}&v=-\sqrt{\nu b}f(\xi,\ \tau),\xi=\sqrt{\frac{b}{\nu}}y,\quad u=bxf_\xi(\xi,\ \tau),\tau=t\omega,\\&\theta(\xi,\tau)=\frac{T-T_\infty}{T_f-T_\infty},\quad \phi(\xi,\tau)=\frac{C-C_\infty}{C_f-C_\infty},J(\xi,\tau)=\frac{\psi-\psi_\infty}{\psi_w-\psi_\infty}.\end{aligned}\right\}\tag{7}$$

In view of above transforms, the simplified system is:

$$\gamma\left(1+\lambda_p\beta\right)f_{\xi\tau}-ff_{\xi\xi}-f_{\xi\xi\xi}+\left(\lambda_p+M\right)f_\xi+f_\xi^2+\beta\begin{pmatrix}\gamma f_{\xi\xi\xi\tau}+2f_\xi f_{\xi\xi\xi}\\-f_{\xi\xi}^2-ff_{\xi\xi\xi\xi}\end{pmatrix}=0,\tag{8}$$

$$\frac{1}{\Pr}(1+R)\theta_{\xi\xi}-\gamma\theta_\tau+f\theta_\xi+Nb\theta_\xi\phi_\xi+Nt(\theta_\xi)^2-\delta_T\begin{pmatrix}\gamma^2\theta_{\tau\tau}+ff_\xi\theta_\xi+f^2\theta_{\xi\xi}\\-2\gamma f\theta_{\xi\tau}-\gamma f_\tau\theta_\xi\end{pmatrix}+\delta\theta=0,\tag{9}$$

$$\phi_{\xi\xi}-\gamma(Sc)\phi_\tau+Scf\phi_\xi+\frac{Nt}{Nb}\theta_{\xi\xi}-\delta_C\begin{pmatrix}\gamma^2\phi_{\tau\tau}+ff_\xi\phi_\xi+f^2\phi_{\xi\xi}\\-2\gamma f\phi_{\xi\tau}-\gamma f_\tau\phi_\xi\end{pmatrix}=0,\tag{10}$$

$$J_{\xi\xi}-S(Lb)J_\tau+LbfJ_\xi-Pe\left[J_\xi\phi_\xi+\phi_{\xi\xi}(J+\sigma_m)\right]=0,\tag{11}$$

The boundary conditions are:

$$\left.\begin{aligned}&f_\xi(0,\ \tau)=\ \sin\tau,\quad f(0,\ \tau)=0,\theta_\xi(0,\ \tau)=-\gamma_a[1-\theta(0,\ \tau)],\ \ \phi_\xi(0,\ \tau)=-\gamma_b[1-\phi(0,\ \tau)],J(0,\ \tau)=1,\\&f_\xi(\infty,\ \tau)\to 0,\ f_{\xi\xi}(\infty,\ \tau)\to 0,\theta(\infty,\ \tau)\to 0,\ \ \phi(\infty,\ \tau)\to 0,J(\infty,\ \tau)\to 0.\end{aligned}\right\}\tag{12}$$

where $\beta=b\Gamma/\nu$ is viscoelastic parameter, $M=\sqrt{\sigma B_0^2/b\rho_f}$ expressing the Hartmann number, $\lambda_p=\nu\varphi/\Omega b$ provides definition of porosity parameter, $R=16\varepsilon T_\infty^3/3kk_a$ is radiated parameter, $\Pr=\nu/\Lambda$ leads to definition of Prandtl number, $\gamma=\varpi/b$ is ratio amongst the oscillating frequency to rate of stretching (ratio parameter), $Nt=\Upsilon D_T(T_f-T_\infty)/T_\infty\nu$ be thermophoresis parameter, $Nb=\Upsilon D_B(C_f-C_\infty)/\Delta C\nu$ the Brownian parameter, ϕ dimensionless concentration, $\delta_T=A_Tb$ is thermal relaxation parameter, $\delta=Q/b(\rho c)_f$ is the heat generation/absorption parameter, $Sc=\nu/D_B$ expresses the Schmidt number, $\delta_C=B_Cb$ used to assessment of concentration relaxation coefficient, $\sigma_m=\psi_\infty/(\psi_w-\psi_\infty)$ is microorganisms concentration difference, $Lb=\nu/D_m$ is bioconvective Lewis number, θ dimensionless temperature, $Pe=\vartheta w/D_m$ Peclet constant, J nondimensional microbes density profile, and $\gamma_a=(h_f/k)\sqrt{\nu/b}$ is the thermal Biot number, $\gamma_b=(k_f/D_B)\sqrt{\nu/b}$ the concentration Biot number.

In order to suggests the applications of sin fraction C_f, Nusselt number Nu, Sherwood number Sh, and motile density number Nn, following relations are imposed [34, 35]:

$$\left.\begin{aligned}&\mathrm{Re}_x^{-1/2}C_f=[f_{\xi\xi}-\beta(3f_\xi f_{\xi\xi}+\gamma f_{\xi\xi\tau}-ff_{\xi\xi\xi})]_{\xi=0},\\&\frac{Nu}{\sqrt{\mathrm{Re}_x}}=-(1+R)\theta_\xi(0,\tau),\ \frac{Sh}{\sqrt{\mathrm{Re}_x}}=-\phi_\xi(0,\tau),\ \frac{Nn}{\sqrt{\mathrm{Re}_x}}=-J_\xi(0,\tau).\end{aligned}\right\}\tag{13}$$

3. Numerical computations by finite difference method (FDM)

The equations given in (8–11) are complex PDEs. Due to the intricate nature of modeled PDEs, numerical calculation presents an intriguing challenge. The equations have been solved using the implicit finite difference method (FDM). In order to initiate the simulations, first the physical problem is truncated from semi-infinite interval $\xi \in [0, \infty)$ into finite boundary $\zeta \in [0,\ 1]$ as follows [36–39]:

$$\left.\begin{aligned}
&\xi = \frac{1}{\zeta} - 1,\\
&\frac{\partial}{\partial \xi} = -\zeta^2 \frac{\partial}{\partial \zeta},\\
&\frac{\partial^2}{\partial \xi^2} = \zeta^4 \frac{\partial^2}{\partial \zeta^2} + 2\zeta^3 \frac{\partial}{\partial \zeta},\\
&\frac{\partial^2}{\partial \xi \partial \tau} = -\zeta^2 \frac{\partial^2}{\partial \zeta \partial \tau},\\
&\frac{\partial^3}{\partial \xi^3} = -\zeta^6 \frac{\partial^3}{\partial \zeta^3} - 6\zeta^5 \frac{\partial^2}{\partial \zeta^2} - 6\zeta^4 \frac{\partial}{\partial \zeta},\\
&\frac{\partial^4}{\partial \xi^3 \partial \tau} = -\zeta^6 \frac{\partial^4}{\partial \zeta^3 \partial \tau} - 6\zeta^5 \frac{\partial^3}{\partial \zeta^2 \partial \tau} - 6\zeta^4 \frac{\partial^2}{\partial \zeta \partial \tau},\\
&\frac{\partial^4}{\partial \xi^4} = \zeta^8 \frac{\partial^4}{\partial \zeta^4} + 12\zeta^7 \frac{\partial^3}{\partial \zeta^3} + 36\zeta^6 \frac{\partial^2}{\partial \zeta^2} + 24\zeta^5 \frac{\partial}{\partial \zeta}.
\end{aligned}\right\} \tag{14}$$

Utilizing the above transformations in Eqs. (8–11):

$$\left.\begin{aligned}
&\gamma\left(1 + \lambda_p \beta\right) \frac{\partial^2 f}{\partial \zeta \partial \tau} + 6\beta\zeta^2 \frac{\partial^2 f}{\partial \zeta \partial \tau} + \gamma\beta\zeta^4 \frac{\partial^4 f}{\partial \zeta^3 \partial \tau} + 6\beta\zeta^3 \frac{\partial^3 f}{\partial \zeta^2 \partial \tau} = \left(\zeta^2 + 8\beta\zeta^4\right)\left(\frac{\partial f}{\partial \zeta}\right)^2\\
&+\left(6\zeta^2 - M^2 - \lambda_p - 36\beta f\zeta^4 - 2\zeta f\right) \frac{\partial f}{\partial \zeta} + \zeta^4 \frac{\partial^3 f}{\partial \zeta^3} + \left(6\zeta^2 - \zeta^2 f - 36\beta f\zeta^4\right) \frac{\partial^2 f}{\partial \zeta^2}\\
&+8\beta\zeta^5 \frac{\partial f}{\partial \zeta}\frac{\partial^2 f}{\partial \zeta^2} - \beta\zeta^6 \left(\frac{\partial^2 f}{\partial \zeta^2}\right)^2 + 2\beta\eta^6 \frac{\partial f}{\partial \zeta}\frac{\partial^3 f}{\partial \zeta^3} - 12\zeta^5 \beta f \frac{\partial^3 f}{\partial \zeta^3} - \beta\zeta^6 f \frac{\partial^4 f}{\partial \zeta^4}.
\end{aligned}\right\} \tag{15}$$

$$\left.\begin{aligned}
&\frac{1}{\Pr}(1 + R)\zeta^4 \frac{\partial^2 \theta}{\partial \zeta^2} + 2\zeta^3 \frac{\partial \theta}{\partial \zeta} - \gamma \frac{\partial \theta}{\partial \tau} - f\zeta^2 \frac{\partial \theta}{\partial \zeta} + Nb\zeta^4 \frac{\partial \phi}{\partial \zeta}\frac{\partial \theta}{\partial \zeta} + Nt\zeta^4 \left(\frac{\partial \theta}{\partial \zeta}\right)^2\\
&-\delta_T \left(\begin{matrix} \gamma^2 \dfrac{\partial^2 \theta}{\partial \tau^2} + f\zeta^4 \dfrac{\partial f}{\partial \zeta}\dfrac{\partial \theta}{\partial \zeta} + f^2 \left(\zeta^4 \dfrac{\partial^2 \theta}{\partial \zeta^2} + 2\zeta^3 \dfrac{\partial \theta}{\partial \zeta}\right) \\ -2\gamma f \dfrac{\partial^2 \theta}{\partial \tau \partial \zeta} - \gamma \dfrac{\partial f}{\partial \tau}\dfrac{\partial \theta}{\partial \tau} \end{matrix}\right) + \delta\theta = 0,
\end{aligned}\right\} \tag{16}$$

$$\left.\begin{aligned}
&\zeta^4 \frac{\partial^2 \phi}{\partial \zeta^2} + 2\zeta^3 \frac{\partial \phi}{\partial \zeta} - \gamma(Sc) \frac{\partial \phi}{\partial \tau} - Scf\zeta^2 \frac{\partial \phi}{\partial \zeta} + \frac{Nt}{Nb}\left(\zeta^4 \frac{\partial^2 \theta}{\partial \zeta^2} + 2\zeta^3 \frac{\partial \theta}{\partial \zeta}\right)\\
&-\delta_C \left(\gamma^2 \frac{\partial^2 \phi}{\partial \tau^2} + f\zeta^4 \frac{\partial \theta}{\partial \zeta}\frac{\partial \phi}{\partial \zeta} + f^2 \left(\zeta^4 \frac{\partial^2 \phi}{\partial \zeta^2} + 2\zeta^3 \frac{\partial \phi}{\partial \zeta}\right) - 2\gamma f \frac{\partial^2 \phi}{\partial \zeta \partial \tau} + \gamma \frac{\partial f}{\partial \tau_\tau}\zeta^2 \frac{\partial \phi}{\partial \zeta}\right) = 0,
\end{aligned}\right\} \tag{17}$$

$$\zeta^4 \frac{\partial^2 J}{\partial \zeta^2} + 2\zeta^3 \frac{\partial J}{\partial \zeta} - S(Lb) \frac{\partial \phi}{\partial \tau} - Lbf\zeta^2 \frac{\partial J}{\partial \zeta} - Pe\left[\zeta^4 \frac{\partial J}{\partial \zeta_\xi}\frac{\partial \phi}{\partial \zeta} + \left(\begin{matrix} \zeta^4 \dfrac{\partial^2 \phi}{\partial \zeta^2} \\ +2\zeta^3 \dfrac{\partial \phi}{\partial \zeta} \end{matrix}\right)(J + \sigma_m)\right] = 0, \tag{18}$$

The boundary conditions are transformed into:

$$\left.\begin{array}{l} f_\zeta = -\sin\tau, f = 0, \theta_\zeta = \gamma_a(1-\theta), \phi_\zeta = \gamma_b(1-\phi), \quad J = 0 \quad \text{at} \quad \zeta = 1, \\ f_\zeta = 0, \quad f_{\zeta\zeta} = 0, \ \theta = 0, \quad \phi = 0, \quad J = 0 \quad \text{at} \quad \zeta = 0. \end{array}\right\} \tag{19}$$

Now discretization of system of Eqs. (15–19) for M are series of nodes $\zeta = (\zeta_1, \ \zeta_2, \ldots\ldots, \ \zeta_M) \in (0, \ \ 1)$. The step size is selected as $\Delta\zeta = \frac{1}{M+1}$. The time level $\tau = (\tau^1, \ \ \tau^2, \ldots.)$. The proposed initial conditions are:

$$f(\zeta, \ \tau = 0) = 0, \quad \theta(\zeta, \ \tau = 0) = 0, \quad \phi(\zeta, \ \tau = 0) = 0, \quad J(\zeta, \ \tau = 0) = 0. \tag{20}$$

The semi-implicit time differentiation scheme is developed for $f, \ \ \theta, \ \ \phi,$ and J to guarantee the solving the linear equations for new step $(n+1)$ is solved.

Table 1. Comparison of results for $f_{\xi\xi}(0, \tau)$ with analysis of Zheng *et al.* [40] by keeping $\gamma = 1, \ M = 12$ and $\lambda_p = \beta = 0$.

τ	Zheng *et al.* [40]	Current results
$\tau = 1.5\pi$	11.678656	11.6786585
$\tau = 5.5\pi$	11.678706	11.6787065
$\tau = 9.5\pi$	11.678656	11.6786592

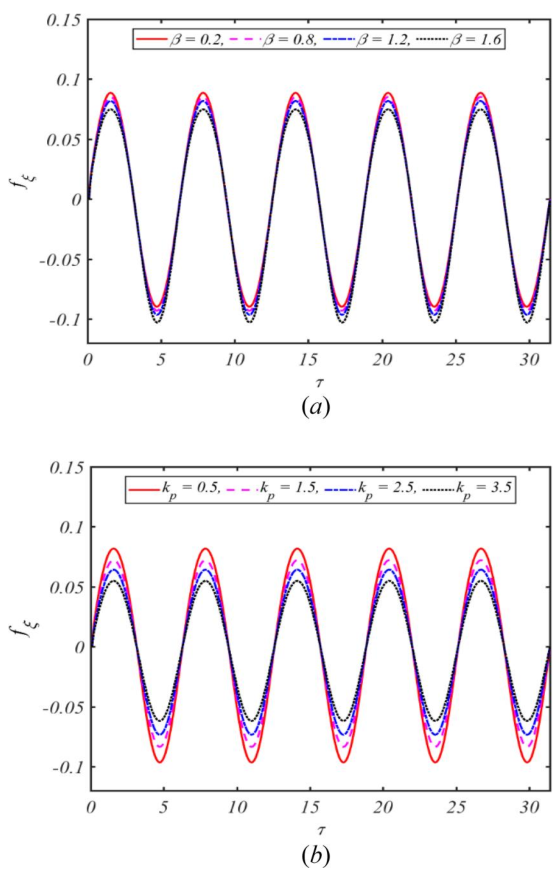

Figure 1. (a, b) Profile of velocity f_ξ with time τ due to (a) β (b) k_p.

4. Validation of numerical results

To analyze the numerical data, we compare the findings in Table 1 with the research conducted by Zheng *et al.* [40]. A remarkable correlation between both outputs has been witnessed.

5. Physical analysis of results

The study of the physical features of a problem involving variations of parameters is both interesting and significant in order to propose diverse applications. The modeled flow issue corresponds to the theoretical flow assumptions, which need graphical analysis of parameters within an established parameter range such as: $0.2 \le \beta \le 1.6$, $0.5 \le k_p \le 3.5$, $0.5 \le M \le 6.0$, $0.1 \le \Pr \le 0.4$, $0.2 \le Sc \le 2.0$, $0.5 \le \delta_T \le 2.0$, $0.5 \le \gamma \le 2.0$, $0.5 \le R \le 2.0$, $0.1 \le Nt \le 1.3$, $0.1 \le Lb \le 1.3$ and $0.1 \le Pe \le 1.0$. Figure 1a examines the variation in velocity f_ξ against time τ subject to distinct values of viscoelastic parameter β. The oscillating variation in f_ξ are predicted under the leading values of β. The magnitude of velocity declined against increasing impact of β. The viscoelastic fluid parameter characterizes the behavior of viscoelastic fluids, which exhibit both elastic and viscous effects in response to deformation rates. Higher values of the viscoelastic parameter indicate a greater dominance of elastic effects, resulting in an increase in fluid velocity. Additionally, periodic oscillations in velocity occur due to the flow over a periodically stretching surface. Figure 1b conveying the illustration of f_ξ due to increasing influence of porosity

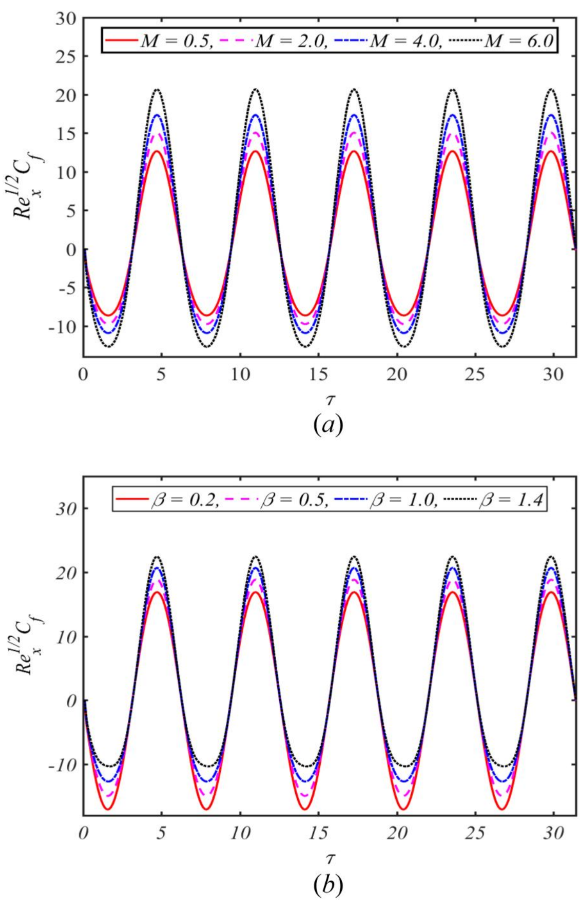

Figure 2. (a, b) Profile of skin friction $\mathrm{Re}_x C_f$ with time τ due to (a) M (b) β.

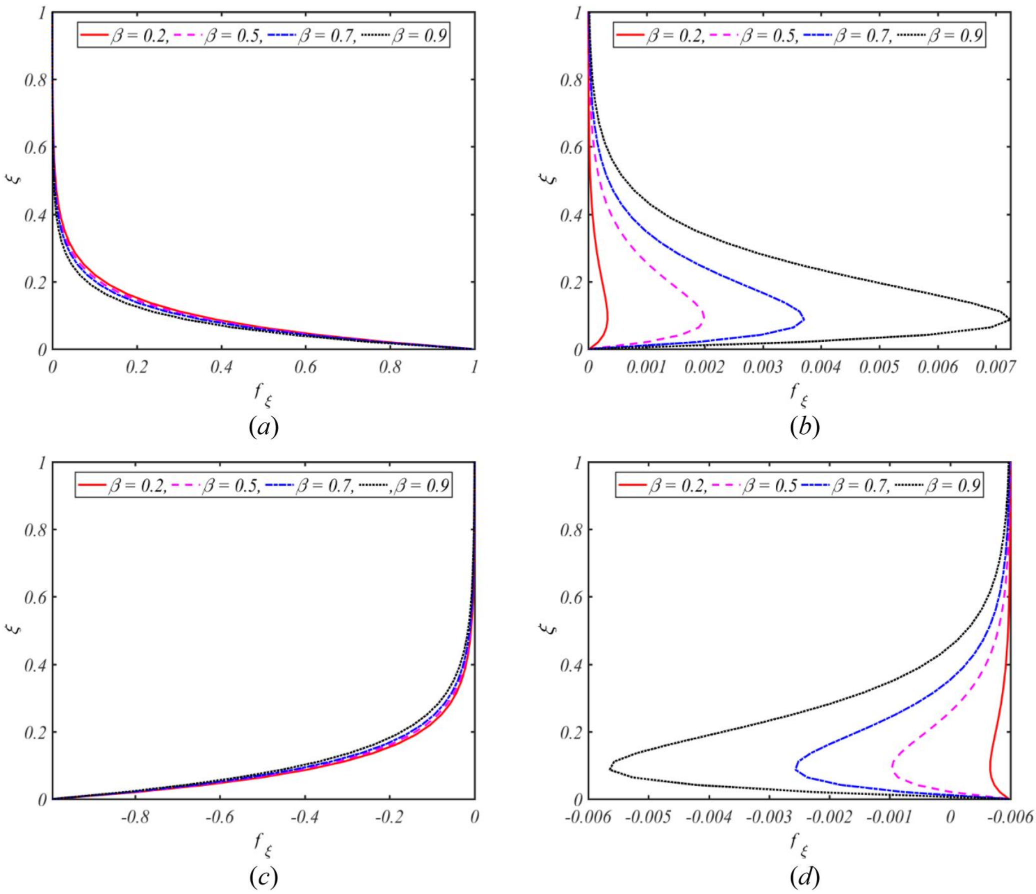

Figure 3. (a–d) Profile of velocity f_ξ due to β at (a) k_p $\tau = 8.5\pi, \tau = 9\pi, \tau = 9.5\pi$ and $\tau = 10\pi$.

parameter k_p. The velocity accelerates uniformly with reducing of magnitude. This reduction in velocity is caused by the permeability of the porous region. These findings play a crucial role in vibrational and control systems. The results illustrated in Figure 2a,*b* presents the significance of skin friction coefficient $\mathrm{Re}_x^{-1/2} C_f$ as a function of time τ under the dominant role of Hartmann number M and viscoelastic parameter β. An oscillation has been preserved in both figures with uniform magnitude. The magnitude of oscillation enhances when large numerical impact is assigned to M and β. The wall shear force is the resistance exerted by fluid particles against a moving plate. Skin friction forces play a crucial part in several technical operations such as pipelines, airplanes, and vehicles. Figure 3a–3*d* has been prepared in order to judge the velocity truncation due to viscoelastic constant β at various time instants. The observations are inspected at four time instant $\tau = 8.5\pi, \tau = 9\pi, \tau = 9.5\pi$ and $\tau = 10\pi$. Here, an oscillations in f_ξ are predicted at $\tau = 9\pi$ and $\tau = 10\pi$. The velocity periodically acceleration at both instants and fluctuation in velocity reaches to 1 asymptotically. However, a linear velocity profile is exhibited at $\tau = 8.5\pi$ and $\tau = 9.5\pi$.

In order to evaluate the variation of Nusselt number Nu by considering the impact of Prandtl number Pr, Figure 4a is prepared. The Nusselt number increases with minor oscillations when Pr get varied. The magnitude of oscillations is very small. Figure 4b concentrates to determination of Sherwood number Sh against Schmidt number Sc. Subject to increasing Sc, an enhancement in Sh is revealed.

Figure 5a–*c* disclosing the analysis for temperature profile θ subject to porosity constant k_p, viscoelastic parameter β, thermal relaxation parameter δ_T, ratio parameter γ, Prandtl number

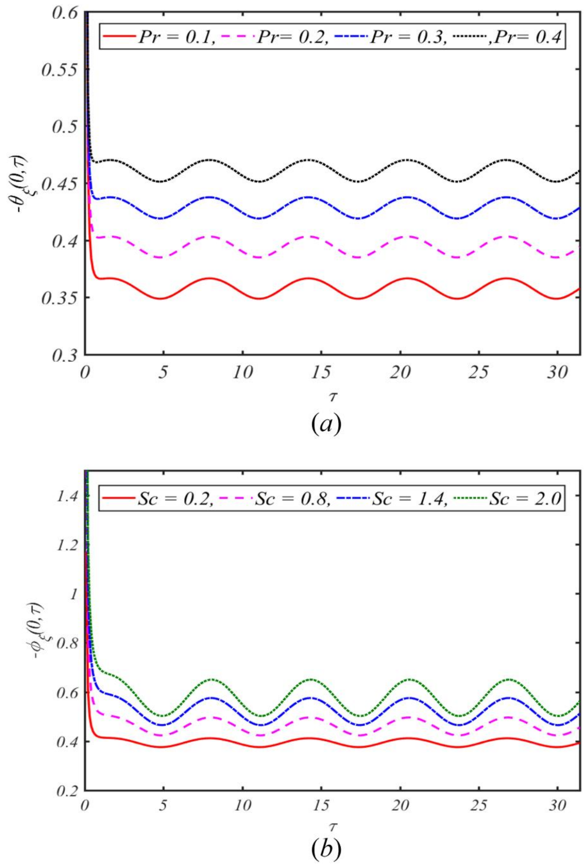

Figure 4. (a, b) (a) Profile of Nusselt number with time τ for Pr (b) profile of S herwood number for *Sc*.

Pr and radiation constant R. Here the analysis is performed at fixed time instant $\tau = \pi/2$. Figure 5a addressing the insight of porosity constant k_p and viscoelastic parameter β. Both parameters lead to growing change in θ. Physically, the improvement in θ due to k_p is associated to permeability of porous space. Heat transport in porous medium has an essential purpose in the fields of petroleum engineering and thermal insulation. Figure 5b contributing to observe the change in θ for thermal relaxation parameter δ_T and ratio parameter γ. The temperature profile reduces for δ_T while increasing observations are noticed for γ. The increasing change in γ leads to improvement in the angular frequency due to which temperature increases. Figure 5c aims to report the change in θ for Prandtl number Pr and radiative constant R. Low temperature profile has resulted due to increment in the Pr. Such decrement in θ is results due to slow truncation in thermal diffusivity.

In order to claim the effective role of involved parameters on concentration profile ϕ, Figure 6a,*b* is reported. The concentration profile gets lower for concentration relaxation number δ_C and Schmidt number *Sc* and explained *via* Figure 6a. The reduction in ϕ due to *Sc* is referred to lower mass diffusivity. Figure 6b announcing the physical prospective of concentration profile ϕ in view of thermophoresis parameter *Nt* and viscoelastic parameter β. The concentration gets boosted when the major role of both parameters has been utilized. The thermophoresis parameter is directly related to the thermophoretic phenomena, which quantifies the movement of nanoparticles in a hot area to a cooler zone. This migration results in an improvement in the concentration profile.

Figure 7a,*b* has been proposed to specify the novel impact of Peclet number *Pe*, bioconvective parameter *Lb*, porosity constant k_p, and viscoelastic coefficient β on microbes density profile *J*. It has been noted that *J* declined for *Pe*, *Lb* and referred to Figure 7a. Slow microbes' density

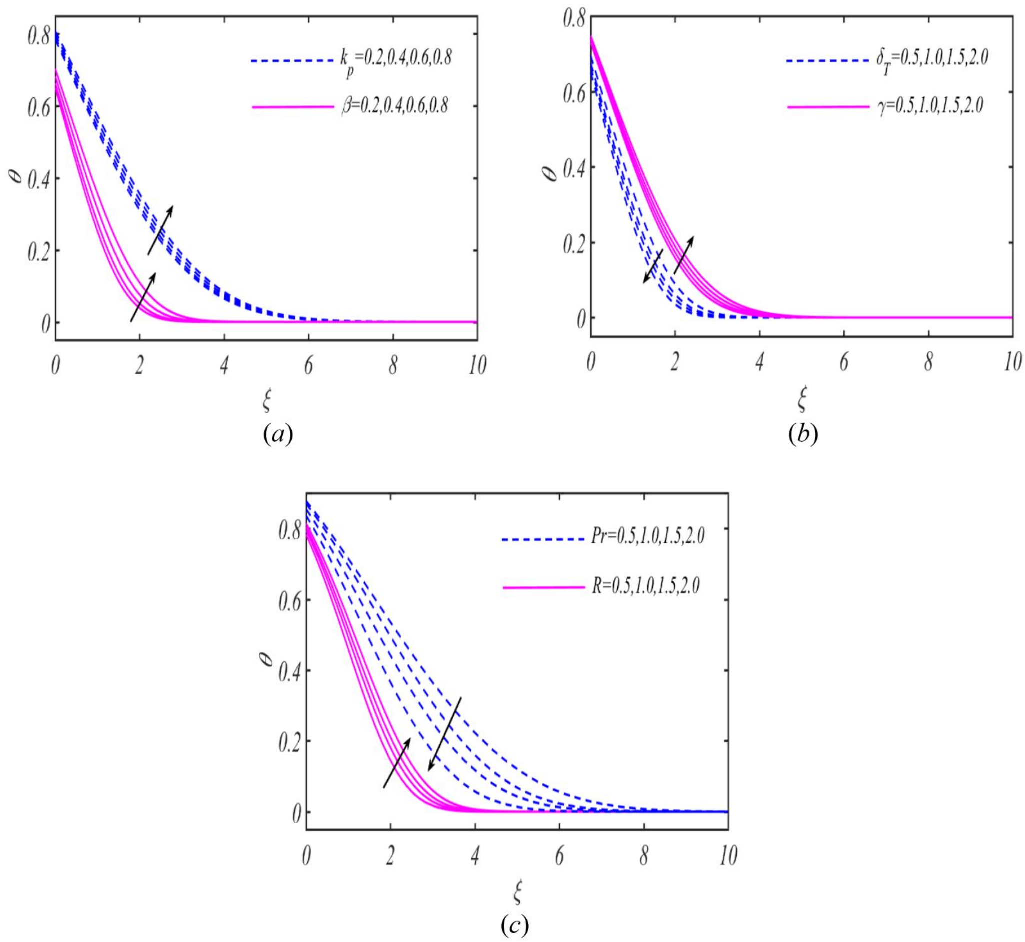

Figure 5. (a–c) Profile of temperature θ due to (a) k_p & β, (b) δ_T & γ, (c) Pr & R.

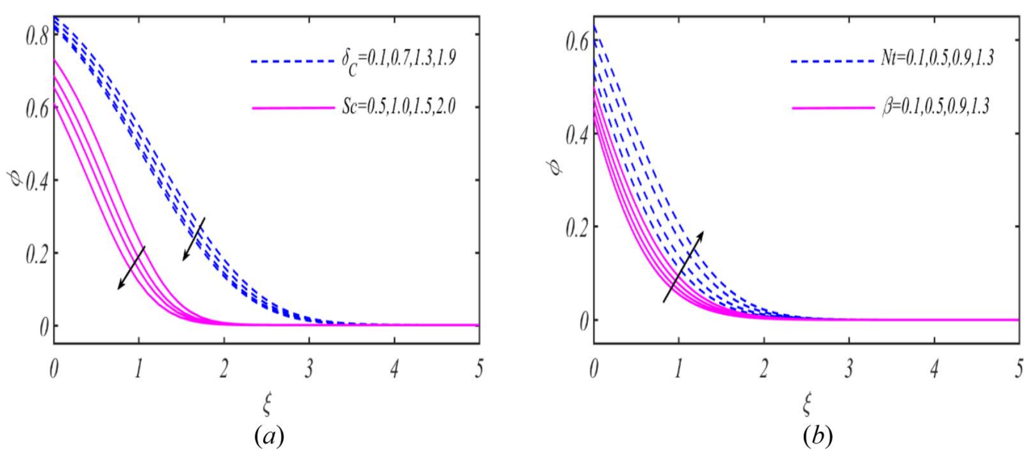

Figure 6. (a, b) Profile of concentration ϕ due to (a) δ_C & Sc, (b) Nt & β.

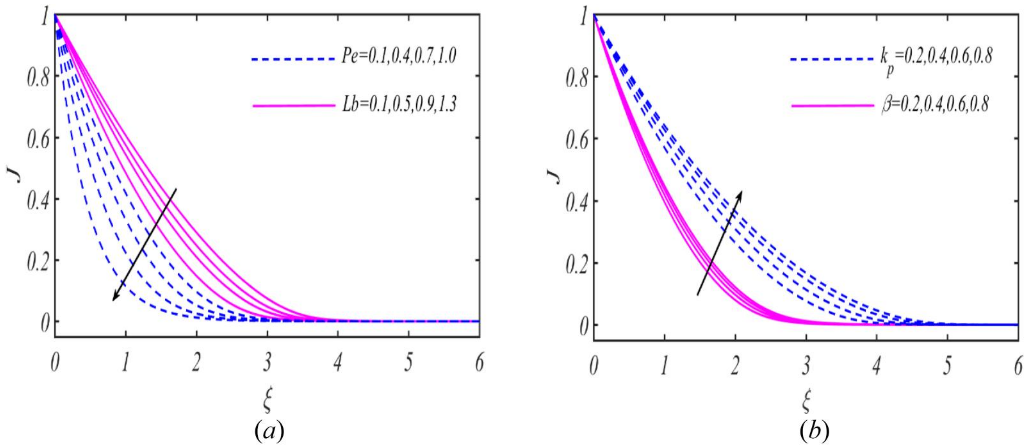

Figure 7. (a, b) Profile of microbes density J due to (a) Pe & β, (b) k_p & β.

profile for Pe. Such outcomes are physically justified due to low motile diffusivity. The bioconvective parameter Lb presents the convective flow of collection of microbes like bacteria in the fluid like water. The role of Lb is important in inspecting the behavior of bioconvection phenomenon. Figure 7b shows that microbes' density profile get peaked change for porosity parameter k_p and viscoelastic parameter β.

6. Conclusion

A study has been conducted on the bioconvective flow of Walters-B nanofluid in the presence of radiative effects caused by an oscillating stretching surface. The CC hypothesis is used to analyze heat and mass transport. The problem is formulated using nonlinear highly ordered PDEs, and the solution is obtained using an implicit finite difference approach. Through graphical analysis, the following observations are derived:

i. A reduction in magnitude of velocity profile is observed due to porosity parameter and viscoelastic constant.
ii. The skin friction coefficient exhibits periodic increases with respect to the Hartmann number.
iii. The Nusselt number increases over time as the Prandtl number varies.
iv. A periodic change in velocity is noted against various of viscoelastic parameter at two different time instants ($\tau = 9\pi$ and $\tau = 10\pi$).
v. The heat transport decreases as a result of the Prandtl number and thermal relaxation parameter.
vi. An increasing shift in the temperature field is seen when the ratio of the oscillating frequency to the stretched rate parameter increases.
vii. Control of concentration field is revealed for concentration relaxation parameter while improvement in concentration is subject to variation of viscoelastic parameter.
viii. The microbe's density profile enhances the presence of porous media and viscoelastic parameters.
ix. Further improvements to the existing model may be made by including other thermal phenomena such as entropy production, viscous dissipation, slip effects, and thermos-diffusion applications. Moreover, these findings may be examined for hybrid nanofluid by using various nanoparticles.

Ethics approval

Not applicable.

Disclosure statement

The authors declare that they have no conflict of interest.

Funding

Not applicable.

ORCID

Sami Ullah Khan http://orcid.org/0000-0001-5826-1279
Adnan http://orcid.org/0000-0003-0071-4743
Arshad Riaz http://orcid.org/0000-0003-0717-6677
Katta Ramesh http://orcid.org/0000-0003-3329-508X
M. M. Bhatti http://orcid.org/0000-0002-3219-7579

Data availability statement

The data that support the findings of this study are available from the corresponding author upon reasonable request.

References

[1] J. Wang, X. Yang, J. J. Klemeš, K. Tian, T. Ma and B. Sunden, "A review on nanofluid stability: preparation and application," *Renew. Sustain. Energy Rev.*, vol. 188, pp. 113854, Dec 2023. DOI: 10.1016/j.rser.2023.113854.

[2] M. K. Mondal, D. Kumar Mandal, N. Biswas, N. K. Manna, K. Al-Farhany and A. J. Chamkha, "Enhanced magneto-convective heat transport in porous hybrid nanofluid systems with multi-frequency nonuniform heating," *J. Magn. Magn. Mater.*, vol. 577, pp. 170794, Jul 2023. DOI: 10.1016/j.jmmm.2023.170794.

[3] F. Mebarek-Oudina *et al.*, "Hydromagnetic flow of magnetite–water nanofluid utilizing adapted Buongiorno model," *Int. J. Mod. Phys. B*, vol. 38, no. 01, pp. 2450003, Jan 2024, DOI: 10.1142/S0217979224500036.

[4] S. Nadeem *et al.*, "Reynolds nano fluid model for Casson fluid flow conveying exponential nanoparticles through a slandering sheet," *Sci. Rep.*, vol. 13, no. 1, pp. 1953, Feb 2023. DOI: 10.1038/s41598-023-28515-1.

[5] M. A. Basit, M. Imran, M. Tahir, A. Eladeb and L. Kolsi, "Numerical analysis of mathematical model for heat and mass transfer through Bioconvective Maxwell nanofluid flow subject to Darcy-Forcheimer and Lorentz forces," *Int. J. Heat Fluid Flow*, vol. 106, pp. 109322, Apr 2024. DOI: 10.1016/j.ijheatfluidflow.2024.109322.

[6] N. Acharya, "Hydrothermal scenario of buoyancy-driven magnetized multi-walled carbon nanotube-Fe3O4-water hybrid nanofluid flow within a discretely heated circular chamber fitted with fins," *J. Magn. Magn. Mater*, vol. 589, pp. 171612, Jan 2024. DOI: 10.1016/j.jmmm.2023.171612.

[7] M. Irfan and M. M. Bhatti, "Effects of Arrhenius kinetic on the magnetized nanofluid flow through a porous stretchable cylinder with slip conditions," *Energy Sources Recovery Util. Environ. Eff.*, vol. 46, no. 1, pp. 1979–1995, Dec 2024. DOI: 10.1080/15567036.2024.2302004.

[8] A. A. Khan, G. Fatima, S. M. Sait and R. Ellahi, "Electromagnetic effects on two-layer peristalsis flow of Powell–Eyring nanofluid in axisymmetric channel," *J Therm. Anal. Calorim.*, vol. 149, no. 8, pp. 3631–3644, Apr 2024. DOI: 10.1007/s10973-024-12907-0.

[9] S. I. Abdelsalam, A. Magesh, P. Tamizharasi and A. Z. Zaher, "Versatile response of a Sutterby nanofluid under activation energy: hyperthermia therapy," *HFF*, vol. 34, no. 2, pp. 408–428, Feb 2024. DOI: 10.1108/HFF-04-2023-0173.

[10] A. Raza, O. V. Stadoleanu, A. M. Abed, A. H. Ali and M. Sallah, "Heat transfer model analysis of fractional Jeffery-type hybrid nanofluid dripping through a poured microchannel," *Int. J. Thermofluid.*, vol. 22, pp. 100656, May 2024. DOI: 10.1016/j.ijft.2024.100656.

[11] P. Praveen Kumar, S. Balakrishnan, A. Magesh, P. Tamizharasi and S. I. Abdelsalam, "Numerical treatment of entropy generation and Bejan number into an electroosmotically-driven flow of Sutterby nanofluid in an asymmetric microchannel," *Numer. Heat Transf. B Fundam.*, pp. 1–20, Mar 2024. DOI: 10.1080/10407790.2024.2329773.

[12] M. Sheikholeslami, Z. Khalili, P. Scardi and N. Ataollahi, "Environmental and energy assessment of photovoltaic-thermal system combined with a reflector supported by nanofluid filter and a sustainable thermoelectric generator," *J. Clean. Prod.*, vol. 438, pp. 140659, Jan 2024. pp. 140659, DOI: 10.1016/j.jclepro.2024.140659.

[13] S. A. Bakar, I. Pop and N. Md Arifin, "Unsteady flow of gyrotactic microorganisms with hybrid nanofluid and higher order slips using modified Buongiorno model," *Int. J. Heat Fluid Flow*, vol. 107, no. 109378, pp. 109378, Jul 2024. DOI: 10.1016/j.ijheatfluidflow.2024.109378.

[14] A. Al-Yaari *et al.*, "The effects of nanofluid thermophysical properties on enhanced oil recovery in a heterogenous porous media," *Case Stud. Chem. Environ. Eng.*, vol. 9, no. 100556, pp. 100556, Jun 2024. DOI: 10.1016/j.cscee.2023.100556.

[15] A. Gholizadeh, M. Pourfallah, M. Gholinia, M. Armin and E. Languri, "The role of nanofluids and fins in a heat exchanger on waste energy recovery from a diesel engine: an experimental and numerical study," *Energy Rep.*, vol. 8, pp. 13353–13368, Nov 2022. DOI: 10.1016/j.egyr.2022.10.009.

[16] S. Shahlaei and M. G. Hassankolaei, "MHD boundary layer of GO–H2O nanoliquid flow upon stretching plate with considering nonlinear thermal ray and Joule heating effect," *Heat Trans. Asian Res.*, vol. 48, no. 8, pp. 4152–4173, Dec 2019. DOI: 10.1002/htj.21586.

[17] S. S. Ghadikolaei, S. Siahchehrehghadikolaei, M. Gholinia and M. Rahimi, "A CFD modeling of heat transfer between CGNPs/H2O Eco-friendly nanofluid and the novel nature-based designs heat sink: hybrid passive techniques for CPU cooling," *Therm. Sci. Eng. Prog.*, vol. 37, pp. 101604, Jan 2023. DOI: 10.1016/j.tsep.2022.101604.

[18] M. M. Bhatti, O. A. Bég and S. Kuharat, "Electromagnetohydrodynamic (EMHD) convective transport of a reactive dissipative carreau fluid with thermal ignition in a non-Darcian vertical duct," *Numer. Heat Transf. A*, pp. 1–31, Nov 2023. DOI: 10.1080/10407782.2023.2284333.

[19] M. Bilal, N. H. Hamad, S. A. AlQahtani and P. Pathak, "Numerical simulation of nanofluid flow across a slender stretching Riga plate subjected to heat source and activation energy," *Numer. Heat Transf. B Fundam.*, pp. 1–14, Apr 2024. DOI: 10.1080/10407790.2024.2337119.

[20] A. Issakhov, Z. Rakhymzhanova and A. Abylkassymova, "Numerical simulation of the effect of height and number of heaters on heat transfer during natural convection in a cubic enclosure filled with nanofluid," *Numer. Heat Transf. A*, vol. 85, no. 15, pp. 2397–2418, Aug 2024. DOI: 10.1080/10407782.2023.2222905.

[21] D. W. Beard and K. Walters, "Elastico-viscous boundary-layer flows I. Two-dimensional flow near a stagnation point," *Math. Proc. Camb. Phil. Soc.*, vol. 60, no. 3, pp. 667–674, Jul 1964. DOI: 10.1017/S0305004100038147.

[22] A. A. Pasha, W. Jamshed, K. A. Juhany, A. Al-Bahi and R. W. Ibrahim, "Computational finite element analysis of electromagnetic radiative nanofluid containing motile germs with chemical reactive process," *Int. J. Mod. Phys. B*, vol. 38, no. 03, pp. 2450038, Jan 2024. DOI: 10.1142/S0217979224500383.

[23] S. N. Rai, B. S. Bhadauria and A. Srivastava, "Study of thermal-instability in nanoliquid (Walter-B viscoelastic) within the Hele-Shaw cell under thermal-modulation using cubic Ginzburg-Landau (GBL) equation," *J. Nanofluids*, vol. 12, no. 8, pp. 2129–2143, Dec 2023. DOI: 10.1166/jon.2023.2079.

[24] S. Vyakaranam, R. Leelavathi, T. S. Rao, V. R. R. Gurrampati, and O. A. Samuel, "Soret-Dufour mechanisms on unsteady boundary layer flow of tangent hyperbolic and Walters-B nanoliquid," *ARFMTS.*, vol. 108, no. 1, pp. 13–27, Sep 2023, DOI: 10.37934/arfmts.108.1.1327.

[25] K. Smida *et al.*, "Lubricated stagnation point flow of Walters-B nanofluid with Cattaneo-Christov heat flux model: hybrid homotopy analysis simulations," *Results Eng.*, vol. 21, pp. 101689, Mar 2024. DOI: 10.1016/j.rineng.2023.101689.

[26] N. Sandeep, R. S. Babu, P. Nanda and G. P. Ashwinkumar, "Enhanced heat transmission in conical slip flow of Walter's-B nanofluid," *Int. J. Mod. Phys. B*, vol. 38, no. 07, pp. 2450096, Mar 2023. DOI: 10.1142/S0217979224500966.

[27] F. Z. Wang, M. Sohail, U. Nazir, E. M. Awwad and M. Sharaf, "Utilization of the Crank-Nicolson technique to investigate thermal enhancement in 3D convective Walter-B fluid by inserting tiny nanoparticles on a circular cylinder," *AIMS Math.*, vol. 9, no. 4, pp. 9059–9090, Mar 2024. DOI: 10.3934/math.2024441.

[28] G. Saini, B. N. Hanumagowda, S. S. K. Raju and S. V. K. Varma, "Nonlinear heat radiation and mass transfer characteristics on MHD Walters' B fluid flow through a porous medium over a stretching sheet," *Partial Differ. Equ. Appl. Math.*, vol. 10, pp. 100699, Jun 2024. DOI: 10.1016/j.padiff.2024.100699.

[29] S. Rehman, Y. Trabelsi, S. Alqahtani, S. Alshehery, S. M., Eldin, Hashim, "A renovated Jaffrey-Hamel flow problem and new scaling statistics for heat, mass fluxes with Cattaneo–Christov heat flux model," Case *Stud. Therm. Eng.*, vol. 43, no.102787, Mar 2023, DOI: 10.1016/j.csite.2023.102787.

[30] R. J. Punith Gowda, R. Naveen Kumar, R. Kumar and B. C. Prasannakumara, "Three-dimensional coupled flow and heat transfer in non-newtonian magnetic nanofluid: an application of Cattaneo-Christov heat flux model," *J. Magn. Magn. Mater.*, vol. 567, pp. 170329, Feb 2023. DOI: 10.1016/j.jmmm.2022.170329.

[31] A. Hussain and Z. Mao, "Heat transfer analysis of MHD Prandtl-Eyring fluid flow with Christov-Cattaneo heat flux model," *Numer. Heat Transf. A*, pp. 1–21, Feb 2024. DOI: 10.1080/10407782.2024.2316208.

[32] M. Saraswathy, D. Prakash, M. Muthtamilselvan and Q. M. Al-Mdallal, "Theoretical study on bio-convection of micropolar fluid with an exploration of Cattaneo–Christov heat flux theory," *Int. J. Mod. Phys. B*, vol. 38, no. 02, pp. 2450016, Jan 2024. DOI: 10.1142/S0217979224500164.

[33] D. Qaiser, Z. Zheng and M. Riaz Khan, "Numerical assessment of mixed convection flow of Walters-B nanofluid over a stretching surface with Newtonian heating and mass transfer," *Therm. Sci. Eng. Prog.*, vol. 22, pp. 100801, May 2021. DOI: 10.1016/j.tsep.2020.100801.

[34] B. R. Kumar and R. Sivaraj, "MHD viscoelastic fluid non-Darcy flow over a vertical cone and a flat plate," *Int. Commun. Heat Mass Transf.*, vol. 40, pp. 1–6, Jan 2013. DOI: 10.1016/j.icheatmasstransfer.2012.10.025.

[35] M. Javed, T. Hayat, M. Mustafa and B. Ahmad, "Velocity and thermal slip effects on peristaltic motion of Walters-B fluid," *Int. J. Heat Mass Transf.*, vol. 96, pp. 210–217, May 2016. DOI: 10.1016/j.ijheatmasstransfer.2015.12.029.

[36] S. Sharma, M. Goyal and A. Dadheech, "Melting, Soret and Dufour effect on MHD Casson fluid flow over a stretching sheet with slip conditions," *J. Eng. Math.*, vol. 146, no. 1, pp. 18, Jun 2024. DOI: 10.1007/s10665-024-10364-0.

[37] M. M. Bhatti, S. Jun, C. M. Khalique, A. Shahid, L. Fasheng and M. S. Mohamed, "Lie group analysis and robust computational approach to examine mass transport process using Jeffrey fluid model," *Appl. Math. Comput.*, vol. 421, pp. 126936, May 2022. DOI: 10.1016/j.amc.2022.126936.

[38] M. M. Bhatti and R. Ellahi, "Numerical investigation of non-Darcian nanofluid flow across a stretchy elastic medium with velocity and thermal slips," *Numer. Heat Transf. B Fundam.*, vol. 83, no. 5, pp. 323–343, May 2023. DOI: 10.1080/10407790.2023.2174624.

[39] A. Paul, J. M. Nath and T. K. Das, "Thermally stratified Cu–Al2O3/water hybrid nanofluid flow with the impact of an inclined magnetic field, viscous dissipation and heat source/sink across a vertically stretching cylinder," *Z Angew. Math. Mech.*, vol. 104, no. 2, pp. e202300084, Feb 2024. DOI: 10.1002/zamm.202300084.

[40] L. C. Zheng, X. Jin, X. X. Zhang and J. H. Zhang, "Unsteady heat and mass transfer in MHD flow over an oscillatory stretching surface with Soret and Dufour effects," *Acta Mech. Sin.*, vol. 29, no. 5, pp. 667–675, Sep 2013. DOI: 10.1007/s10409-013-0066-6.